Available online at www.sciencedirect.com
SCIENCE DIRECT®
Acta Materialia 53 (2005) 2683–2692
Acta MATERIALIA
www.actamat-journals.com

Athermal heterogeneous nucleation of solidification

T.E. Quested, A.L. Greer *

University of Cambridge, Department of Materials Science & Metallurgy, Pembroke Street, Cambridge CB2 3QZ, UK

Received 8 December 2004; received in revised form 21 February 2005; accepted 22 February 2005
Available online 2 April 2005

Abstract

For heterogeneous nucleation of solidification, the conditions for initiation of solid grains on nucleant areas of defined size are analysed. Calculations of the work of formation show that the solid formed on a nucleant area has both metastable- and unstable-equilibrium configurations, which permit analysis of the competition between thermal nucleation (a stochastic process) and athermal nucleation, a deterministic process in which the number of nucleation events depends on the undercooling, but not on time nor on the mechanism (adsorption, wetting or nucleation) of the initial formation of a thin solid layer on the nucleant area. It is concluded that for potent nucleants, initiating grains at small undercooling, athermal nucleation dominates. Thermal nucleation in advance of athermal is negligible, but athermal nucleation can be delayed when solute restricts solid growth.

Keywords: Nucleation; Solidification; Adsorption; Kinetics

1. Introduction

The term athermal nucleation was first used by Fisher et al. [1] in discussing transformations (notably formation of martensite) which are observed not to proceed under isothermal conditions, but only on cooling. It contrasts with thermal nucleation in which thermal activation over a critical work of formation generates nuclei of the new phase at a steady-state rate as the temperature is held constant. Fisher et al. considered the case in which an equilibrium population of sub-critical embryos at a given temperature could be retained by rapid cooling to a lower temperature. In cases where some of the retained population have sizes greater than the critical size at the lower temperature, there is a burst of nucleation, even when the rate of thermal nucleation at that temperature may be negligible. The essence of athermal nucleation, as noted by Fisher et al. [1] is that sub-critical embryos are "automatically promoted to nuclei" when, on cooling, the critical size decreases and sweeps past their own size. The role of athermal nucleation has been considered in cases as diverse as the martensitic transformation in steel [2] and crystallization of polymers [3,4].

The rate of athermal homogeneous nucleation, analysed by Ziabicki [5], is proportional to the cooling rate, and therefore likely to dominate at high cooling rate. Im et al. [6] noted its importance for pulsed-laser melted thin films of silicon cooled at $\geqslant 10^{10}\,\mathrm{K\,s^{-1}}$, and proposed a nucleation-mechanism diagram to identify the regimes of quench rate and undercooling in which thermal or athermal nucleation would be dominant. For rapid quenches, however, the quasi-steady-state approximation breaks down, and transient effects tend to reduce the number of nuclei [7]. Shneidman [8] has analysed the competition between such transient effects and true athermal nucleation which increases the number of nuclei when there is no further evolution of the embryo size distribution. He refined the nucleation-mechanism map of Im et al. and noted that athermal

* Corresponding author. Tel.: +44 1223 334308; fax: +44 1223 334567.
E-mail address: alg13@cam.ac.uk (A.L. Greer).

1359-6454/$30.00
doi:10.1016/j.actamat.2005.02.028

homogeneous nucleation is significant only for the combination of extremely high cooling rate and large undercooling.

In solidification, the nucleation of the crystalline phase is, however, almost always heterogeneous. In this case, an athermal contribution to the nucleation rate can be significant over a wide range of conditions. For example, in the freezing of a cast iron, Oldfield [9] found that the number of grains per unit volume n was independent of holding time at a given undercooling, but proportional to the square of the undercooling ΔT. An athermal nucleation law of this type is easy to implement in numerical modelling of solidification and is widely used. As proposed by Thévoz et al. [10], the nucleation rate $dn/d\Delta T$ as a function of ΔT is commonly taken to have a Gaussian form; this has been used in probabilistic modelling of realistic grain structures [11]. The form of $dn/d\Delta T$ is not intrinsic to the liquid, but dependent on thermal history. In particular, as reviewed by Turnbull [12], the extent to which a melt can be undercooled may increase strongly with the degree to which it was superheated above its liquidus temperature T_L. This can be explained as an effect of the survival of embryos of the crystalline phase above T_L in cavities (conical or cylindrical, in a mould wall or other substrate) [12]. If the superheat is greater, fewer embryos survive and the survivors are in cavities with a smaller mouth; the ΔT at which they become active nuclei on cooling is inversely proportional to the mouth radius [12]. (Similar analyses have been applied for the nucleation of gas bubbles in supersaturated liquids. Pre-existing bubbles in cavities are active nuclei if the cavity mouth exceeds a critical radius [13].)

Turnbull [14] showed that dispersions of mercury droplets could be used to measure the rate of homogeneous nucleation under isothermal conditions, but he found that the large ΔT required was not always obtainable. In some dispersions (presumed to be contaminated with mercury oxide) the droplet undercoolings before solidification were only 2–4 K [15]. For these dispersions, the fraction of droplets solidified was dependent on ΔT but not on time. Turnbull attributed this to athermal nucleation at surface patches acting as potent catalysts. He noted that a embryo of the crystalline phase formed on such a patch could become an active transformation nucleus only when, on cooling, the critical nucleation radius r^* becomes less than the radius of the patch. On this basis, he was able to derive the size distribution of patches from the distribution of ΔT values at which the droplets solidified.

Similar athermal heterogeneous nucleation occurs in the solidification of inoculated aluminium alloys [16]. Inoculation with an Al–Ti–B master alloy contributes particles of TiB_2 to the melt, and nucleation on these is dominant. The particles are hexagonal prisms and nucleation of solid aluminium is on their flat {0001} faces [17]. Measured undercoolings are consistent with grain initiation occurring when r^* falls below the radius r_N of the {0001} faces (hexagonal, but approximated as circles) and a pre-existing thin layer of solid aluminium on the {0001} faces then grows outwards. This appearance of a transformation nucleus has been termed the onset of free growth [16]. By measuring the distribution of r_N, it is possible to model the sequence of grain initiation events on cooling and to make quantitatively correct predictions of final grain size as a function of refiner addition level, alloy solute content and cooling rate [16]. The success of this free-growth model has prompted studies of how the particle size distributions in inoculants might be optimized [18].

In this paper we analyse further the heterogeneous nucleation of solidification on nucleant substrates of a defined size. The standard approach to finite-size effects, taken by Fletcher [19–21], considers nucleant particles of various shapes, but analyses only the rate of thermal nucleation under isothermal conditions. We extend this work by analysing athermal nucleation. For simplicity we consider nucleant areas that are plane circles of radius r_N, the analysis for more complicated shapes mostly differing only by geometrical factors. Plane circular areas of nucleant can equally represent the surface patches considered by Turnbull [15] (Fig. 1(a)), or the active faces of nucleant particles (Fig. 1(b)), for example the {0001} faces of TiB_2 inoculant particles used to

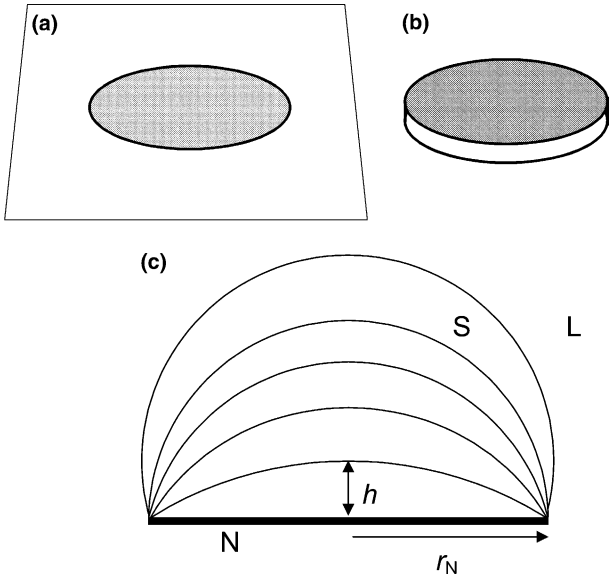

Fig. 1. Examples (shaded in (a) and (b)) of circular nucleant areas of the kind considered in this work: (a) a surface patch, (b) the active face of a nucleant particle. The growth of solid from such a nucleant area (c) involves an increase in the curvature of the liquid/solid interface enabled by an increase in undercooling. The curvature is maximum when the liquid/solid interface is hemispherical and there is free growth beyond that point. The onset of free growth as the undercooling is increased constitutes athermal heterogeneous nucleation of solidification.

grain-refine aluminium. Athermal nucleation on such areas is illustrated in Fig. 1(c). At a given undercooling, solid may be formed on the substrate, but the lateral spread of the solid is limited by the nucleant area. The solid takes the form of a spherical cap, and the extent of its growth can be represented by the height h. As h increases, the radius of curvature r_{LS} of the liquid/solid interface decreases. Such growth stops when r_{LS} has decreased to equal r^*, the critical nucleation radius for the ambient undercooling ΔT. For small ΔT, it is readily derived [22] that

$$r^* = \frac{2\gamma_{LS}}{\Delta S_V \Delta T}, \tag{1}$$

where γ_{LS} is the free energy per unit area of the liquid/solid interface and ΔS_V is the entropy of fusion per unit volume. The solid can be described as dormant; it is not yet a nucleus for solidification of the entire liquid. For such dormant solid, it is expected that $r_{LS} = r^*$. If the undercooling is increased, r^* decreases, permitting further growth. When r^* has decreased to equal r_N the solid has the form of a hemisphere ($h = r_N$) and r_{LS} is at a minimum. At this point the solid is no longer dormant, since further growth causes a favourable increase in r_{LS} and free growth permits solidification of the entire liquid. The critical undercooling ΔT_{fg} for the onset of free growth is obtained from Eq. (1):

$$\Delta T_{fg} = \frac{2\gamma_{LS}}{\Delta S_V r_N}. \tag{2}$$

By calculating the work of formation of solid on defined circular areas at undercoolings less than and greater than ΔT_{fg}, we examine the nature of athermal nucleation and the transition between thermal and athermal nucleation (i.e., between stochastic and deterministic behaviour). In particular, we test the assumption that effective nucleation of solidification is at ΔT_{fg}, rather than occurring earlier on cooling because of thermal fluctuation, or later because kinetic limitations force r_{LS} to deviate from r^*. First, however, we consider the different possibilities for the initial formation of solid.

2. Initial formation of solid

Heterogeneous nucleation of solidification on a substrate is conventionally considered in terms of the classical model with a solid embryo in the form of a spherical cap (Fig. 2(a)) making a contact angle θ with the substrate. Defining free energies γ_{SN} for the solid/nucleant interface and γ_{LN} for the liquid/nucleant interface, θ is given by

$$\gamma_{LN} = \gamma_{SN} + \gamma_{LS}\cos\theta, \tag{3}$$

where it is important to note that θ is defined only when $\gamma_{LS} \geqslant |\gamma_{LN} - \gamma_{SN}|$. The radius of curvature of the liquid/solid interface for a critical nucleus in the form of a spherical cap is identical to that for the spherical nucleus in homogeneous nucleation. The work of formation of the spherical-cap nucleus W^*_{hetero} is, however, reduced compared to that for the spherical nucleus in the homogeneous case W^*, in proportion with the reduced solid volume [22]:

$$W^*_{hetero} = W^* f(\theta), \quad \text{where } f(\theta) = \tfrac{1}{4}(2 - 3\cos\theta + \cos^3\theta). \tag{4}$$

The effects of the line tension around the perimeter of a spherical-cap embryo have been analysed for condensation from vapour [23,24], but have not generally been considered for solidification of melts. In any case, line-tension effects are significant only for small r^*, and are negligible at the small undercoolings of interest in the present work.

The spherical-cap model is expected to have difficulties in the case of most interest, that of potent nucleation when θ is small. When $\theta \leqslant 10°$, the nucleus would be less than one atomic monolayer thick [25], and the spherical-cap geometry is a bad description. It is then better to model embryos as a monolayer discs [26]. Among the studies indicating difficulties with the analysis of nucleation at low θ are those on the undercoolings required for onset of solidification in entrained liquid droplets. The spherical-cap nucleation model provides a reasonable fit to observed kinetics when $\theta \geqslant 40°$ and correspondingly the undercooling to achieve heterogeneous nucleation is large ($\Delta T > 50$ K) [27,28]. On the other hand, for smaller θ and smaller ΔT, the classical model is unable to fit the observed kinetics with reasonable parameters [29,30]. Coudurier et al. [31] suggested that heterogeneous nucleation might be treated as adsorption of a solid-like layer on the substrate, and this concept

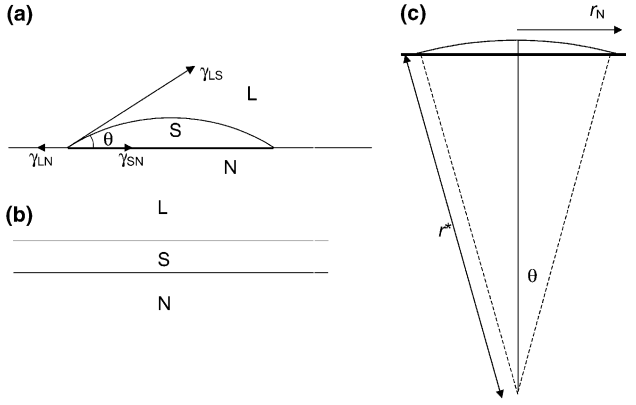

Fig. 2. (a) A classical spherical-cap heterogeneous embryo of solid, with contact angle θ determined by the balance of interfacial energies; (b) the "wetting" of the nucleant area by the solid which occurs when $\gamma_{LS} + \gamma_{SN} < \gamma_{LN}$; (c) an example of a critical heterogeneous nucleus illustrating that for a potent nucleant (small θ), the critical radius for nucleation r^* can exceed the radius r_N of the nucleant area.

has been considered in detail to interpret results such as those on the entrained droplets [32,33]. In the model usually considered, there is a critical undercooling beyond which it is thermodynamically favourable for there to be atom-by-atom adsorption forming a solid layer on the substrate.

The formation of an adsorbed solid-like monolayer at a critical undercooling is distinct from stabilization of an identifiable solid layer by "wetting" of the substrate. In terms of interfacial energies, we can distinguish two cases:

Case I $\gamma_{LS} + \gamma_{SN} < \gamma_{LN}$
Case II $\gamma_{LS} + \gamma_{SN} > \gamma_{LN}$

In case I (Fig. 2(b)), there is no solution to Eq. (3), and it is thermodynamically favourable for the nucleant to be wetted by the solid at all temperatures below the liquidus temperature T_L, and a layer of solid is stabilized even above T_L; there is no critical undercooling for the appearance of the solid layer. In case II, an undercooling is required for nucleation of the solid. The nucleant is not wetted by the solid, and formation of a thin solid layer covering the nucleant would be energetically less favourable than the formation of spherical-cap embryos of solid (Fig. 2(a)).

Conventional analyses emphasise case II and classical spherical-cap nuclei. Case I has been largely overlooked because it appears to suggest that there is no nucleation barrier to solidification, even though, as noted in Section 1, a wetting layer of solid may be dormant with a free-growth barrier to its becoming a transformation nucleus. However, case I was considered in early work on the effect of thermal history on undercooling of liquids; Richards [34] suggested that a crystalline adsorbate might exist on substrates. This idea was pursued in the particular case of TiB_2 inoculant particles in aluminium, where the hypernucleation theory considered the conditions for forming a quasi-solid nucleant layer on the surface of the particles above the liquidus temperature [35,36]. There is indeed some microscopical evidence for a layer on these particles [17]. Transmission electron microscopy has recently been used [37] to show that there can be ordering in liquids at substrate surfaces, even above T_L.

For the effective nucleation temperature to be given by Eq. (2) according to the model depicted in Fig. 1(c), there must be initial formation of solid on the nucleant substrate and either of the cases identified above can apply. In case I the solid exists as a thin layer even above T_L and there is no nucleation barrier for formation of this initial solid. It is likely to form even when the cooling rate is very high. In case II, the solid must be nucleated on the substrate and this occurs beyond a critical undercooling; accepting that there are geometrical problems for small θ, the spherical-cap model is taken as the general description of this case. Fig. 2(c) shows schematically a critical spherical-cap nucleus on a substrate with radius r_N. The radius of the nucleus base is $r^* \sin\theta$, where r^* is the critical radius of curvature of the liquid/solid interface. Provided $r^* \sin\theta < r_N$, as shown, a nucleus of the expected shape can be formed. The probability of nucleus formation is reduced at higher cooling rates. As noted in Section 1, growth of the solid outward from the nucleant area encounters a barrier if $r_N < r^*$. This barrier disappears if the undercooling exceeds the free-growth undercooling ΔT_{fg} (Eq. (2)).

Fig. 3 shows the regimes of nucleation behaviour as a function of reduced undercooling ($\Delta T/\Delta T_{fg}$, the value of ΔT_{fg} being set by the r_N of the substrate) and contact angle θ. In regime (i), the nucleant area is too small to permit a spherical-cap nucleus to form on it. In regime (ii), a spherical-cap nucleus can form but its growth stops when it has spread over the nucleant area and thickened such that the radius of curvature of the liquid/solid interface has decreased to r^*. The borderline between regimes (i) and (ii) is given by

$$\frac{\Delta T}{\Delta T_{fg}} = \sin\theta. \tag{5}$$

In regime (iii) $r_N > r^*$ and there is no barrier to free growth; in this case, the rate-limiting step for effective nucleation (i.e., for the substrate to act as a transformation nucleus for solidification of the liquid) is the initial formation of solid on the substrate.

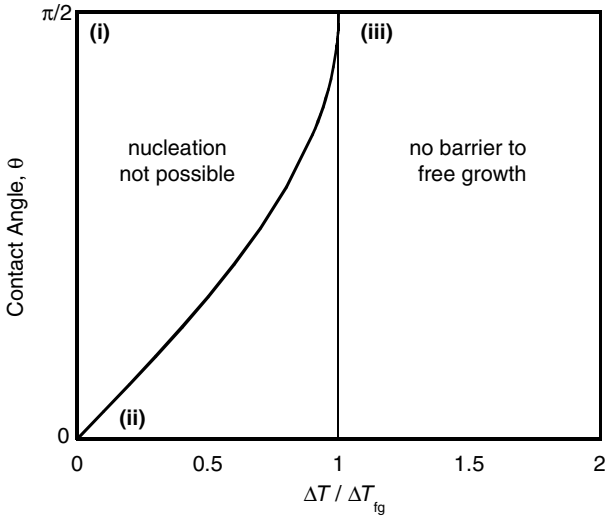

Fig. 3. Regimes of nucleation behaviour as a function of reduced undercooling ($\Delta T/\Delta T_{fg}$) and contact angle θ. In (i), the nucleant area is too small to permit a spherical-cap nucleus to form. In (ii), the regime of most interest in the present work, a nucleus can form but its growth stops when it has spread over the nucleant area and thickened such that the liquid/solid interface reaches the critical radius of curvature r^*. The case of solid formed by adsorption or wetting can be represented by $\theta = 0$. In (iii), $r_N > r^*$, there is no barrier to free growth, and the rate-limiting step for effective nucleation is the initial formation of solid on the substrate.

In regime (ii), with low θ it is easy to nucleate solid on the substrate. Case I in which the interfacial energies ensure that there is a solid layer even above T_L, can be represented on Fig. 3 by $\theta = 0$. In either case, the dormant solid does not lead to transformation of the liquid until the undercooling is increased into regime (iii). The kinetics of effective nucleation depend on the free-growth barrier and the cooling from regime (ii) to regime (iii); they do not depend on the mechanism (adsorption, wetting, or spherical-cap nucleation) of formation of the initial solid.

3. Analysis of nucleation

3.1. Work of formation of the solid cap

We consider the growth of a spherical cap of solid covering a nucleant area of radius r_N (Fig. 1(c)). The balance of interfacial energies underlying Eq. (3) does not apply and (in contrast to earlier analyses [19–21]), there is no defined contact angle. Another consequence of complete coverage of the nucleant area is that line tension plays no rôle. For the cap, the radius of curvature of the liquid/solid interface r_{LS} is related to the height of the cap h by

$$r_{LS} = \frac{h}{2} + \frac{r_N^2}{2h}. \tag{6}$$

The volume of the cap, V_{cap} is given by

$$V_{cap} = \pi\left(r_{LS}h^2 - \frac{h^3}{3}\right) = \pi\left(\frac{r_N^2 h}{2} + \frac{h^3}{6}\right) \tag{7}$$

and the area of the liquid/solid interface A_{LS} by

$$A_{LS} = 2\pi r_{LS}h = \pi\left(h^2 + r_N^2\right). \tag{8}$$

The work required to form a cap of solid (W_{cap}) has contributions from interfacial energies and from the free energy change associated with the solidification of the volume V_{cap}. Consistent with there being pre-existing solid, the reference point for energy ($W_{cap} = 0$) is taken to be that of an infinitesimally thin layer of solid coating the entire nucleant area. The only relevant interfacial energy is then $A_{LS}\gamma_{LS}$. Consistent with the derivation of Eq. (1), the free energy of fusion per unit volume is taken to be $\Delta S_V \Delta T$, an excellent approximation for small ΔT. The work of cap formation,

$$W_{cap} = \gamma_{LS}\left(A_{LS} - \pi r_N^2\right) - V_{cap}\Delta S_V \Delta T, \tag{9}$$

by substituting from Eqs. (7) and (8), can be expressed as

$$W_{cap} = \gamma_{LS}\pi h^2 - \Delta S_V \Delta T\left(\frac{\pi h^3}{6} + \frac{\pi r_N^2 h}{2}\right). \tag{10}$$

The universal form of W_{cap} is best presented in terms of dimensionless quantities. In doing so, a given shape of solid cap should correspond to a given dimensionless undercooling. The dimensionless cap height is taken to be h/r_N. The dimensionless undercooling is obtained by scaling with respect to the free-growth undercooling (Eq. (2)); thus athermal nucleation occurs when the dimensionless undercooling $\Delta T/\Delta T_{fg} = 1$. A dimensionless work of formation can be obtained by normalizing with respect to $W^*_{\Delta T_{fg}}$, the critical work for homogeneous nucleation of a sphere at the free-growth undercooling ΔT_{fg}:

$$W^*_{\Delta T_{fg}} = \frac{16\pi\gamma_{LS}^3}{3\Delta S_V^2 \Delta T_{fg}^2} = \frac{4\pi\gamma_{LS}r_N^2}{3}. \tag{11}$$

Rearranging Eq. (10) in terms of these dimensionless quantities gives

$$\frac{W_{cap}}{W^*_{\Delta T_{fg}}} = -\frac{1}{4}\left(\frac{\Delta T}{\Delta T_{fg}}\right)\left(\frac{h}{r_N}\right)^3 + \frac{3}{4}\left(\frac{h}{r_N}\right)^2 - \frac{3}{4}\frac{\Delta T}{\Delta T_{fg}}\frac{h}{r_N}. \tag{12}$$

The form of Eq. (12) is plotted in Fig. 4 for five values of dimensionless undercooling. For $\Delta T < \Delta T_{fg}$, the work of cap formation passes through a minimum followed by a maximum as h/r_N is increased. These extrema occur at

$$\frac{h}{r_N} = \left(\frac{\Delta T_{fg}}{\Delta T} \pm \sqrt{\left(\frac{\Delta T_{fg}}{\Delta T}\right)^2 - 1}\right) \tag{13}$$

and represent conditions of equilibrium across the liquid/solid interface. At these points the radius of curvature of that interface has the critical value r^* given by Eq. (1), expressed in dimensionless terms as

$$\frac{r^*}{r_N} = \frac{\Delta T_{fg}}{\Delta T}. \tag{14}$$

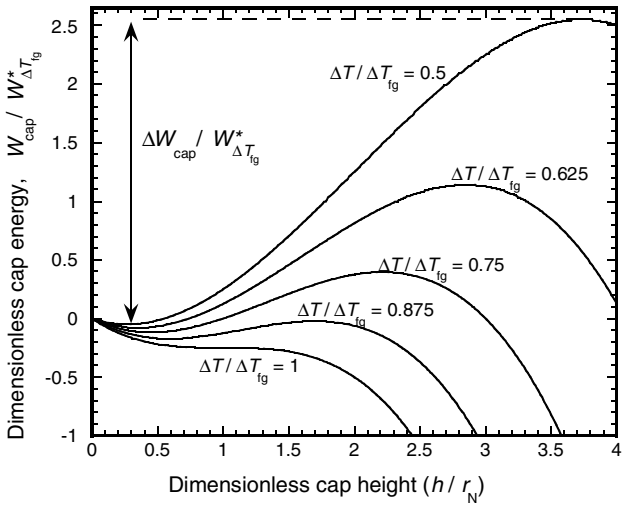

Fig. 4. Dimensionless work of formation ($W_{cap}/W^*_{\Delta T_{fg}}$) of the solid cap as a function of dimensionless cap height (h/r_N) plotted for various values of dimensionless undercooling ($\Delta T/\Delta T_{fg}$) (Eq. (12)). The work of formation is normalized with respect to the critical work for homogeneous nucleation at the free-growth undercooling. The minima (maxima) in these energy curves represent metastable (unstable) equilibrium configurations.

Geometrically (Fig. 5), the solid caps on the nucleant area are obtained by cutting a sphere of equilibrium curvature with a plane such that the circle of intersection has a radius equal to r_N. The cap of smaller volume (a) is in metastable equilibrium; the larger cap (b) is in unstable equilibrium.

The work of formation and r_{LS} are presented in Fig. 6 for the case of $\Delta T/\Delta T_{fg} = 0.5$. Between the two equilibrium conditions shown in Fig. 5, $r_{LS} < r^*$. The work of cap formation in this figure is normalized with respect to $W^*_{\Delta T}$ the critical work for homogeneous nucleation at the *actual* undercooling:

$$W^*_{\Delta T} = \frac{16\pi\gamma_{LS}^3}{3\Delta S_V^2 \Delta T^2}. \quad (15)$$

This normalization would not be useful in Fig. 4, since $W^*_{\Delta T}$ would vary from curve to curve, but it is useful for the given undercooling in Fig. 6 in indicating how the work of cap formation compares with the critical work for homogeneous nucleation.

Fig. 4 shows that for $\Delta T/\Delta T_{fg} < 1$, there is an energy barrier for nucleation. As the normalization is with respect to the fixed quantity $W^*_{\Delta T_{fg}}$, the energies on the different curves can be compared directly. As the dimensionless undercooling is increased, the two extrema converge and the barrier decreases. At $\Delta T/\Delta T_{fg} = 1$, the work of formation as a function of cap height no longer exhibits extrema; there is just the stationary point at

$$h = r_{LS} = r^* = \frac{2\gamma_{LS}}{\Delta S_V \Delta T} \quad (16)$$

when the solid takes the form of a hemisphere and there is no barrier to free growth (Fig. 4). Cooling through the condition $\Delta T/\Delta T_{fg} = 1$ gives athermal nucleation. At $\Delta T/\Delta T_{fg} < 1$, there could be thermal activation over the nucleation barrier, and we now assess the likelihood of this pre-empting athermal nucleation on cooling.

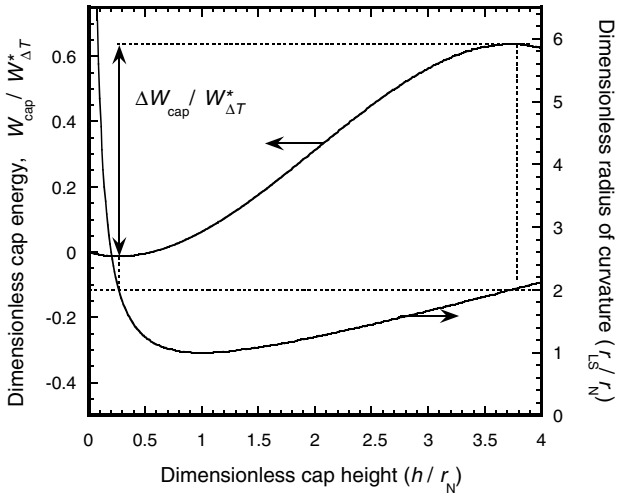

Fig. 6. The dimensionless work of formation (W_{cap}/W^*) of the solid cap and radius of curvature of the liquid/solid interface (r_{LS}/r_N) as a function of the dimensionless cap height (h/r_N) at a dimensionless undercooling of 0.5 (Eq. (10)). The work of formation is normalized with respect to the critical work for homogeneous nucleation at the actual undercooling (Eq. (15)). A dimensionless undercooling of 0.5 results in a dimensionless critical radius of 2 (dashed line), which is the value at the extrema on the work curve. The critical work for free growth (ΔW_{cap}) is the energy difference between the extrema and is less than the critical work for homogeneous nucleation.

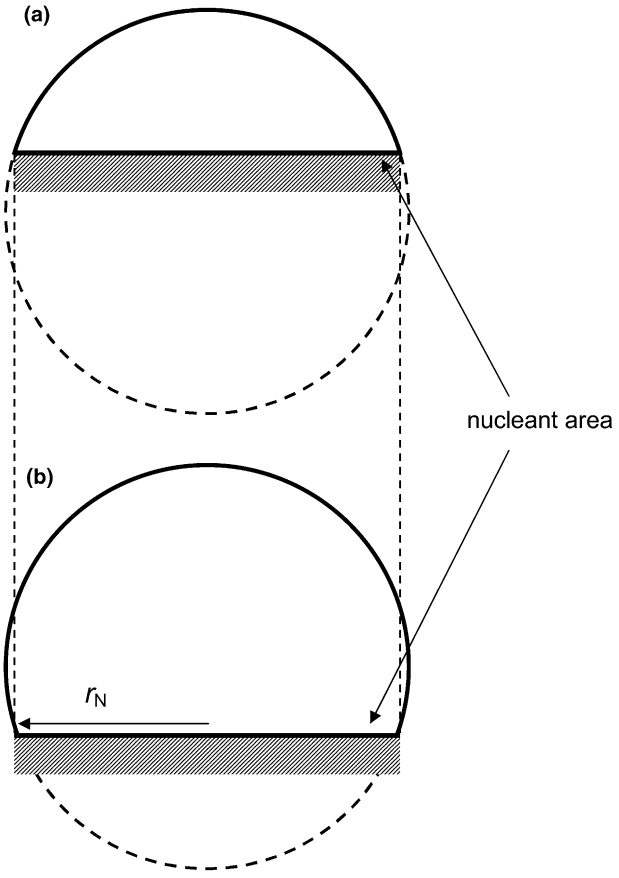

Fig. 5. The (a) metastable- and (b) unstable-equilibrium configurations of the dormant-solid cap for $\Delta T < \Delta T_{fg}$. The radius of curvature of the liquid/solid interface in each case has the critical value r^* and the two configurations are geometrically related.

3.2. The competition between thermal and athermal nucleation

The initial, infinitesimally thin, coating of solid on the nucleant area grows naturally to the metastable and dormant condition shown in Fig. 5(a). From that condition, the critical work of thermal nucleation ΔW_{cap} is the difference in energy between the two extrema, which can be expressed in dimensionless terms as

$$\frac{\Delta W_{cap}}{W^*_{\Delta T_{fg}}} = \left[\left(\frac{\Delta T_{fg}}{\Delta T}\right)^2 - 1\right]\sqrt{1 - \left(\frac{\Delta T}{\Delta T_{fg}}\right)^2} \quad (17)$$

or

$$\frac{\Delta W_{\mathrm{cap}}}{W^*_{\Delta T}} = \left[1 - \left(\frac{\Delta T}{\Delta T_{\mathrm{fg}}}\right)^2\right]^{3/2}. \quad (18)$$

The ratio $\Delta W_{\mathrm{cap}}/W^*_{\Delta T}$ tends to 1 (or 0) as $\Delta T/\Delta T_{\mathrm{fg}}$ tends to 0 (or 1). For the case shown in Fig. 6 ($\Delta T/\Delta T_{\mathrm{fg}} = 0.5$), $\Delta W_{\mathrm{cap}}/W^*_{\Delta T} = 0.65$, showing that, as expected, the barrier is less than for homogeneous nucleation. The critical work for thermal nucleation (Eq. (17)) is plotted (on a logarithmic scale, given its range of values) as a function of the dimensionless undercooling in Fig. 7, and shows a sharp transition. For small $\Delta T/\Delta T_{\mathrm{fg}}$, the dimensionless work $\Delta W_{\mathrm{cap}}/W^*_{\Delta T_{\mathrm{fg}}} \gg 1$, while for large $\Delta T/\Delta T_{\mathrm{fg}}$, the work $\Delta W_{\mathrm{cap}}/W^*_{\Delta T_{\mathrm{fg}}} \ll 1$. The likelihood of thermal activation over this energy barrier depends on the ratio of the barrier height to the thermal energy $k_{\mathrm{B}}T$ (where k_{B} is Boltzmann's constant and T is the temperature). The critical value of this ratio has been evaluated for different cases. For homogeneous nucleation of solidification, for example, the detectable onset is when $W^* = (60 \pm 2)k_{\mathrm{B}}T$ [38]. In the present case, however, we are concerned with the probability of surmounting the energy barrier on a given nucleant area rather than anywhere in the volume of liquid. Following the arguments of Feder et al. [39] for the random nature of atomic exchange with embryos/nuclei of near-critical size, thermal activation and athermal growth become indistinguishable when the energy barrier $\Delta W_{\mathrm{cap}} \leqslant k_{\mathrm{B}}T$. Taking $\Delta W^*_{\Delta T_{\mathrm{fg}}}$ from Eq. (11), the condition for significant thermal activation of nucleation, before the free-growth criterion is met, is

$$\frac{\Delta W_{\mathrm{cap}}}{W^*_{\Delta T_{\mathrm{fg}}}} \leqslant \frac{3k_{\mathrm{B}}T}{4\pi\gamma_{\mathrm{LS}}r_{\mathrm{N}}^2}. \quad (19)$$

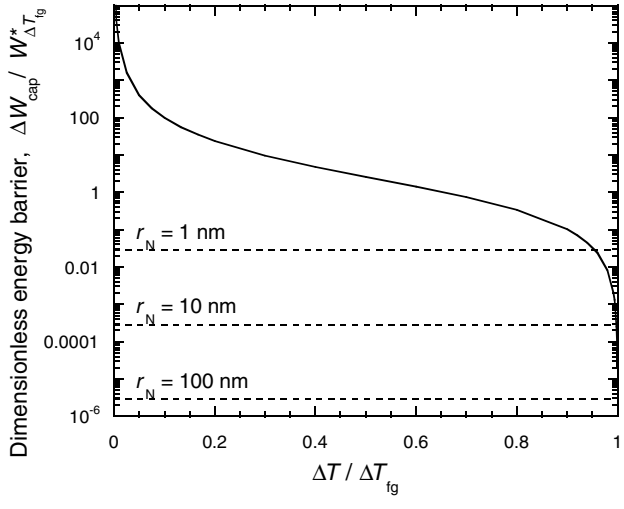

Fig. 7. The dimensionless critical work for free growth ($\Delta W_{\mathrm{cap}}/W^*_{\Delta T_{\mathrm{fg}}}$) as a function of dimensionless undercooling ($\Delta T/\Delta T_{\mathrm{fg}}$) (Eq. (17)). The dashed lines indicate values of the critical work below which thermal activation of nucleation is likely to precede athermal nucleation on cooling. These values depend on the radius of the nucleant area (Eq. (19), with substitution for $T_{\mathrm{M}}/\gamma_{\mathrm{LS}}$ typical for metals).

The condition depends on the size of the nucleant area and the ratio T/γ_{LS}. As the undercoolings of interest are small, we take T to be the melting temperature T_{M}. For metallic elements γ_{LS} and T_{M} are roughly proportional (a compilation of data can be found, for example, in Ref. [38]), with $\gamma_{\mathrm{LS}}/T_{\mathrm{M}} \approx 1.2 \times 10^{-4}\ \mathrm{J\ m^{-2}\ K^{-1}}$. Substituting this ratio into Eq. (19), values of $\Delta W_{\mathrm{cap}}/\Delta W^*_{\Delta T_{\mathrm{fg}}}$ are obtained for selected values of r_{N}. When the main curve in Fig. 7 falls below a given contour, thermal nucleation is likely to be significant. It can be seen that thermal nucleation is significant only at large dimensionless undercoolings when $\Delta T/\Delta T_{\mathrm{fg}}$ approaches one. It is more significant for smaller nucleant areas, but even for the smallest area considered, with $r_{\mathrm{N}} = 1$ nm, thermal nucleation would be significant only for $\Delta T/\Delta T_{\mathrm{fg}} > 0.95$. In the real case of inoculation of aluminium using an Al–Ti–B master alloy, the TiB_2 particles on which grain nucleation occurs have {0001} faces with r_{N} typically not smaller than 1.5 μm. In such a case, thermal nucleation is significant only for $(1 - \Delta T/\Delta T_{\mathrm{fg}}) < 5 \times 10^{-8}$. Thus the assumption made in earlier modelling work [16] that the condition for grain initiation would be that given by Eq. (2) is fully justified. For micrometre-sized nucleant areas, thermal nucleation is negligible in advance of the free-growth condition (Eq. (2)) being met on cooling. Thus the effective nucleation of solid is completely deterministic and governed by temperature change; it is not stochastic.

3.3. Kinetic effects on athermal nucleation

In considering athermal nucleation at the onset of free growth on cooling, we have assumed that the dormant solid is in its metastable equilibrium configuration in which $r_{\mathrm{LS}} = r^*$. As r^* decreases on cooling, this requires the cap height h to increase. From Eq. (13), the increase of h is given by

$$\frac{\mathrm{d}h/r_{\mathrm{N}}}{\mathrm{d}(\Delta T)/\Delta T_{\mathrm{fg}}} = \left(\frac{\Delta T_{\mathrm{fg}}}{\Delta T}\right)^2 \left(\frac{\Delta T_{\mathrm{fg}}}{\Delta T}\frac{1}{\sqrt{(\Delta T_{\mathrm{fg}}/\Delta T)^2 - 1}} - 1\right) \quad (20)$$

and this has the form shown in Fig. 8. Assuming that the liquid is cooled at a constant rate $\dot{T}$, the rate of increase of h with respect to time t is

$$\frac{\mathrm{d}h}{\mathrm{d}t} = \dot{T}\frac{\mathrm{d}h}{\mathrm{d}\Delta T} = \dot{T}r_{\mathrm{N}}\frac{\Delta T_{\mathrm{fg}}}{\Delta T^2}\left(\frac{\Delta T_{\mathrm{fg}}}{\Delta T}\frac{1}{\sqrt{(\Delta T_{\mathrm{fg}}/\Delta T)^2 - 1}} - 1\right). \quad (21)$$

Both this rate and $\mathrm{d}h/\mathrm{d}\Delta T$ (Fig. 8) diverge to infinity as ΔT approaches ΔT_{fg}. It is thus impossible for the dormant cap always to maintain its metastable configuration. The rate of increase in cap height may be limited

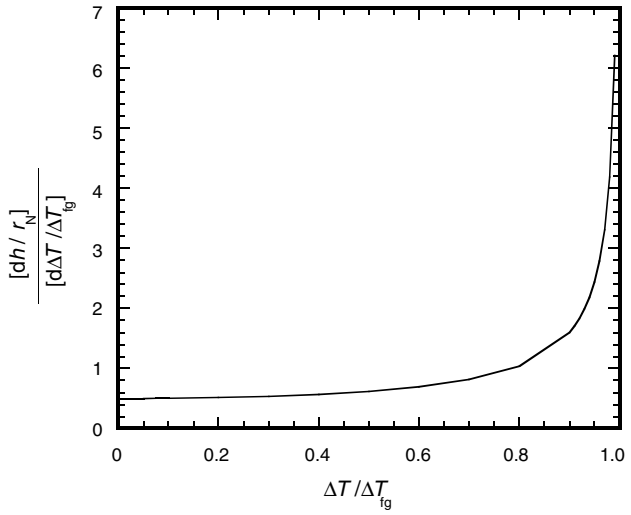

Fig. 8. The rate of change of metastable-equilibrium cap height with undercooling plotted against undercooling. All parameters are normalized to be dimensionless. Given kinetic limits on the velocity of the liquid/solid interface, the divergence of the rate of change of cap height as $\Delta T/\Delta T_{fg}$ approaches one implies that the metastable-equilibrium configuration cannot be maintained, inhibiting athermal nucleation.

by several factors: the kinetics of interfacial atomic rearrangement, transport of heat and transport of solute. In typical alloy solidification at least, the most important of these is the transport of solute, the difficulty of which can be quantified by the solutal undercooling ΔT_{sol}. If ΔT_{sol} is a significant fraction of the total undercooling, the undercooling available to sustain curvature of the liquid/solid interface is reduced and the effective value of r^* is increased, inhibiting the attainment of the free-growth condition. We arbitrarily take ΔT_{sol} to be significant if it exceeds 10% of the total undercooling. As dh/dt tends to infinity as $\Delta T/\Delta T_{fg}$ tends to 1, ΔT_{sol} always becomes significant in this way. We examine whether it is significant at $\Delta T/\Delta T_{fg} = 0.9$; if so, athermal nucleation is likely to be detectably more difficult than expected from the earlier analysis.

When the liquid/solid interface approaches a hemispherical shape, the growth of the solid can be approximated by the invariant-size approximation for solute diffusion around a growing sphere of radius h

$$\frac{dh}{dt} = \frac{D_{sol}\Delta T_{sol}}{rQ}, \tag{22}$$

where D_{sol} is the diffusivity of the solute in the liquid [16]. For a binary alloy the growth-restriction parameter Q is given by [16]

$$Q = m(k-1)C_0, \tag{23}$$

where m is the liquidus slope, k is the equilibrium partition coefficient, and C_0 is the solute content in the liquid. Substituting $\Delta T/\Delta T_{fg} = 0.9$ into Eq. (21) and rearranging yields

$$\frac{dh}{dt} = 1.6\frac{\dot{T}}{\Delta T_{fg}} r_N. \tag{24}$$

Substituting for ΔT_{fg} from Eq. (2) and equating to Eq. (22) yields

$$\Delta T_{sol} = \frac{0.8\dot{T} r_N^3 Q \Delta S_V}{D_{sol}\gamma_{LS}}. \tag{25}$$

Comparing this to the total undercooling at the free-growth condition yields

$$\frac{\Delta T_{sol}}{\Delta T_{fg}} = \frac{0.2\dot{T} r_N^4 Q \Delta S_V^2}{D_{sol}\gamma_{LS}^2}. \tag{26}$$

Setting $\Delta T_{sol}/\Delta T_{fg} \geqslant 0.1$ as the condition for kinetic effects to be significant, we derive an expression for the nucleant-area radius sufficient to cause significant deviation from the metastable configuration of dormant solid and therefore inhibition to athermal nucleation:

$$r_N \geqslant \left[\frac{D_{sol}\gamma_{LS}^2}{2\dot{T}Q\Delta S_V^2}\right]^{1/4}. \tag{27}$$

To evaluate typical magnitudes we take the example of aluminium alloys inoculated with Al–Ti–B master alloy. Even for commercial-purity aluminium, transport of solute is the main inhibitor of solid growth [16,40]. Substituting $D_{sol} = 2.52\times10^{-9}$ m^2 s^{-1}, $\Delta S_V = 1.112\times10^6$ J K^{-1} m^{-3}, and $\gamma_{LS} = 158$ mJ m^{-2} (values for aluminium alloys as used in [16]) into Eq. (27) gives

$$r_N \geqslant \frac{1.9\times10^{-6}}{\sqrt[4]{\dot{T}Q}}. \tag{28}$$

Substituting typical values of Q (in K) and $\dot{T}$ (in K s^{-1}) into this equation reveals that the critical r_N (in m) is close to the radius of the TiB_2 inoculant particles present in the melt. For a low solute level ($Q = 2.2$ K) typical of an inoculated commercial-purity aluminium and a cooling rate typical of DC ingots (3.5 K s^{-1}), r_N is 1.15 μm; for the same cooling rate but $Q = 20$ K, $r_N = 0.65$ μm. As the smallest r_N of TiB_2 particles typically active in nucleating grains [16] is 1.5 μm, some kinetic effects are expected.

3.4. Non-planar nucleant areas

The calculations of the work of formation of the solid cap are for the case of a planar nucleant area, but can easily be modified for other cases. For example, the formation of solid on a concave nucleant area is followed by growth. At $\Delta T = 0$ the metastable equilibrium configuration of the liquid/solid interface is planar across the mouth of the cavity, a condition for which $h = 0$ can be defined. For $0 < \Delta T < \Delta T_{fg}$, the solid grows to the same metastable equilibrium as already identified. The description of the work of formation of the solid on a concave nucleant area then simply requires that the curves in Figs. 4 and 6 be extended to negative values of h. As the relative energies of the extrema are not af-

fected, the work of formation ΔW_{cap} is unaffected. This case of a concave area can be applied, as originally analysed by Turnbull [12], to solid in a cavity in a substrate, if the outer surface of the substrate is not wetted by the solid.

The case of a convex nucleant area is dealt with simply by starting the curves in Figs 4 and 6 at the value of h corresponding to the degree of convexity; the work is not defined for smaller values of h. The work of formation of the solid cap is unaffected provided the minimum value of h is less than that of the energy minimum; otherwise the work is reduced. The convexity of the area, however, inhibits the formation on it (by classical heterogeneous nucleation, adsorption or wetting) of the initial layer of solid.

4. Conclusions

Athermal nucleation occurs when sub-critical embryos become active nuclei on cooling because the critical size decreases and sweeps past their own size. It is commonly considered for solid-state transformations, particularly for the nucleation of martensite. For solidification, however, previous studies have been limited and focused on homogeneous nucleation, for which athermal effects are significant only at extremes of high cooling rate and large undercooling. The present work shows that, in contrast, for the more usual case of heterogeneous nucleation of solidification, athermal nucleation is likely to be dominant. This facilitates solidification modelling by providing a nucleation law in which the number of grains is a function of undercooling, but not of time.

The initial formation of solid on nucleant areas may be by adsorption, wetting, or classical heterogeneous nucleation of a spherical cap. Particularly for potent nucleants, the solid is formed at undercoolings where the critical nucleation radius r^* is significantly greater than r_N the radius of the nucleant area. The solid is therefore dormant (unable to lead to overall solidification) until the critical undercooling is reached at which $r^* = r_N$. The undercooling ΔT_{fg} for effective nucleation of a solid grain is then given by the conditions for free-growth set by r_N; it is unaffected by the mechanism of the initial solid formation.

The energetics of formation of dormant solid on nucleant areas have been analysed. The analysis presented for planar areas can readily be adapted for concave and convex areas. The energy of formation of dormant solid as a function of the thickness (height) of the solid on the nucleant area shows a minimum, which marks the extent of natural growth of the solid, and a maximum which is the barrier to thermal nucleation. This barrier disappears as the undercooling approaches ΔT_{fg}. For nucleant areas of reasonable size (of the order of $r_N = 1$ μm), it is found that the probability of thermal nucleation preceding athermal on cooling is negligible. On the other hand, athermal nucleation may be delayed to larger undercooling by kinetic effects arising from solute restriction of solid growth.

Overall the calculations justify the use of the free-growth criterion in modelling conventional solidification processing, such as inoculation to achieve grain refinement of aluminium alloys.

Acknowledgement

TEQ is supported by an EPSRC CASE studentship associated with Alcan Inc.

References

[1] Fisher JC, Hollomon JH, Turnbull D. J Appl Phys 1948;19:775.
[2] Ghosh G, Olsen GB. Acta Metall Mater 1994;42:3361.
[3] Sajkiewicz P. J Polym Sci B 2002;40:1835.
[4] Sajkiewicz P. J Polym Sci B 2003;41:68.
[5] Ziabicki A. J Chem Phys 1968;48:4374.
[6] Im JS, Gupta VV, Crowder MA. Appl Phys Lett 1998;72:662.
[7] Kelton KF, Greer AL. J Non-Cryst Solids 1986;79:295.
[8] Shneidman VA. J Appl Phys 1999;85:1981.
[9] Oldfield W. Trans ASM 1966;59:945.
[10] Thévoz Ph, Desbiolles JL, Rappaz M. Metall Trans A 1989;20A:311.
[11] Rappaz M, Gandin Ch-A. Acta Metall Mater 1993;41:345.
[12] Turnbull D. J Chem Phys 1950;18:198.
[13] Jones SF, Evans GM, Galvin KP. Adv Colloid Interf Sci 1999;80:27.
[14] Turnbull D. J Chem Phys 1952;20:411.
[15] Turnbull D. Acta Metall 1953;1:8.
[16] Greer AL, Bunn AM, Tronche A, Evans PV, Bristow DJ. Acta Mater 2000;48:2823.
[17] Schumacher P, Greer AL, Worth J, Evans PV, Kearns MA, Fisher P, et al. Mater Sci Technol 1998;14:394.
[18] Quested TE, Greer AL. Acta Mater 2004;52:3859. & 5233.
[19] Fletcher NH. J Chem Phys 1958;29:572.
[20] Fletcher NH. J Chem Phys 1959;31:1136.
[21] Fletcher NH. J Chem Phys 1963;38:237.
[22] Christian JW. The theory of transformations in metals and alloys. 2nd ed. Oxford: Pergamon; 1975. p. 418–475.
[23] Navascués G, Tarazona P. J Chem Phys 1981;75:2441.
[24] Talanquer V, Oxtoby DW. J Chem Phys 1996;104:1483.
[25] Cantor B. Phil Trans Roy Soc Lond A 2003;361:409.
[26] Stranski IN, Kaischew R. Z Chem B 1934;26:100.
[27] Kim WT, Zhang DL, Cantor B. Metall Trans A 1991;22A:2487.
[28] Kim WT, Cantor B. J Mater Sci 1991;26:2868.
[29] Kim WT, Cantor B. Acta Metall 1992;40:3339.
[30] Kim WT, Cantor B. Acta Metall Mater 1994;42:3045.
[31] Coudurier L, Eustathopoulos N, Desré P, Passerone A. Acta Metall 1978;26:465.
[32] Cantor B. Mater Sci Eng A 1994;178:225.
[33] Kim WT, Cantor B. Acta Metall Mater 1994;42:3115.

[34] Richards WT. J Am Chem Soc 1932;54:479.
[35] Jones GP. In: Solidification technology in the foundry and cast house. London: The Metals Society; 1983. p. 112–4.
[36] Jones GP. In: Beech J, Jones H, editors. Solidification processing 1987. London: The Institute of Metals; 1988. p. 496–9.
[37] Donnelly SE, Birtcher RC, Allen CW, Morrison I, Furuya K, Song M, et al. Science 2002;296:507.
[38] Kelton KF. Solid State Phys 1991;45:75.
[39] Feder J, Russell KC, Lothe J, Pound GM. Adv Phys 1966;15:111.
[40] Quested TE, Dinsdale AT, Greer AL. Acta Mater 2005;53:1323.